



SAPIENZA
UNIVERSITÀ DI ROMA

Evidence for Oscillation of Atmospheric Neutrinos

Unraveling the transformation of μ -neutrinos into τ -neutrinos
through Super-kamiokande Collaboration results

By Lorena Bucuru

Neutrinos

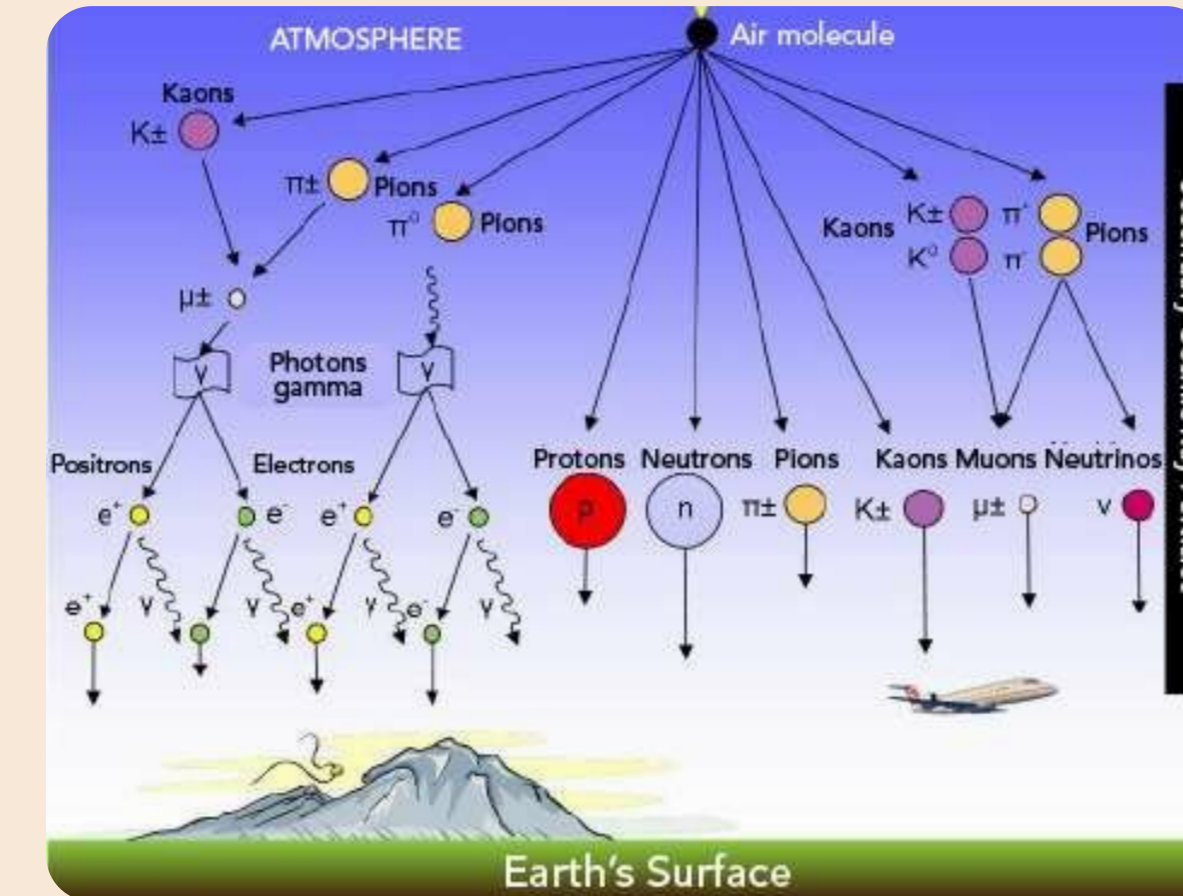


- Fundamental particles, leptons.
- No electric charge.
- Interact weakly with matter.
- Three types.
- Can be detected indirectly via interactions in large detectors.

Atmospheric Neutrinos

How are they produced?

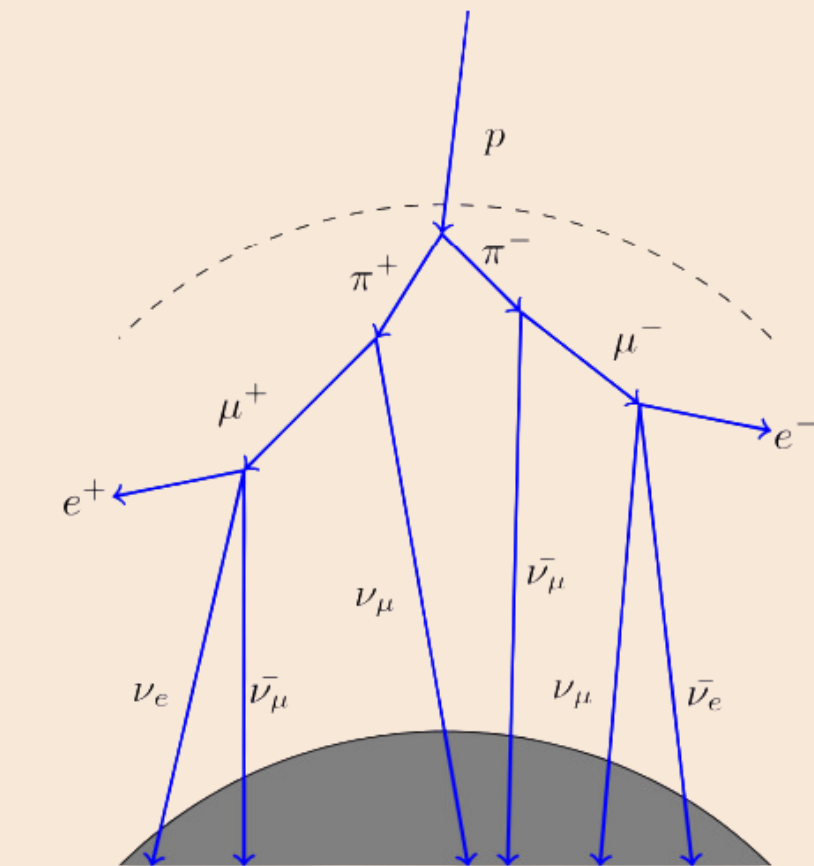
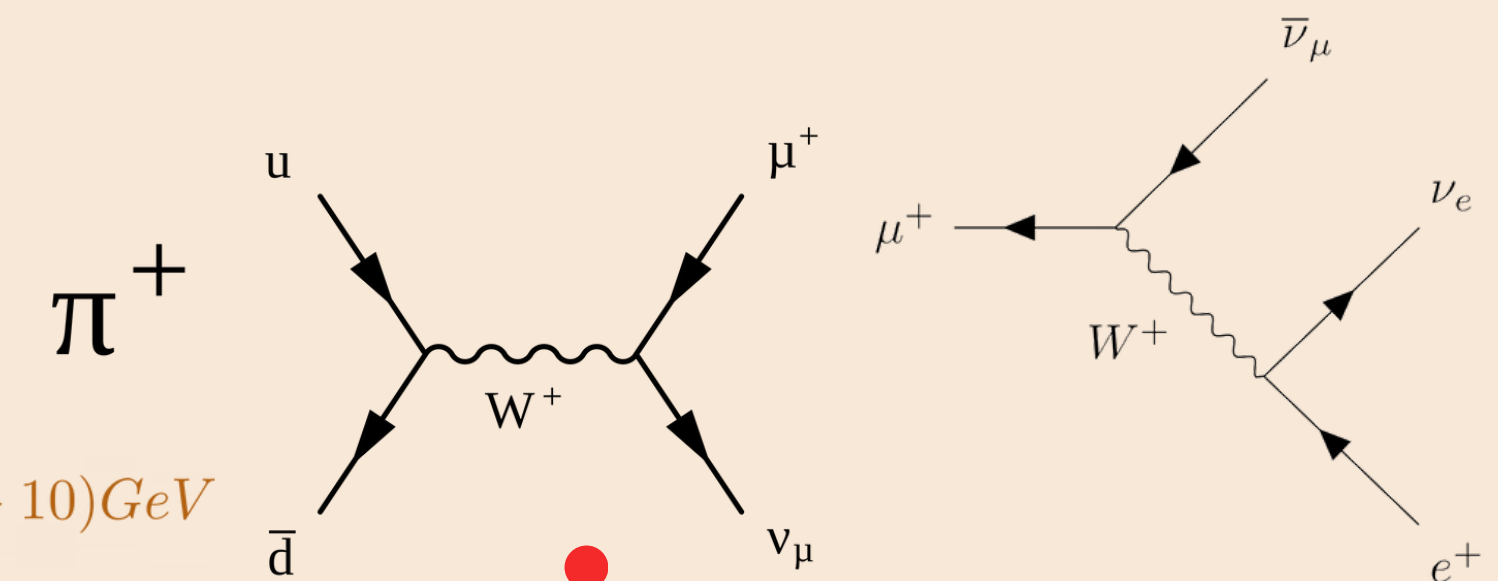
Produced when cosmic rays collide with Earth's atmosphere, creating pions and kaons, which decay into muon and electron neutrinos.



How many do we expect?

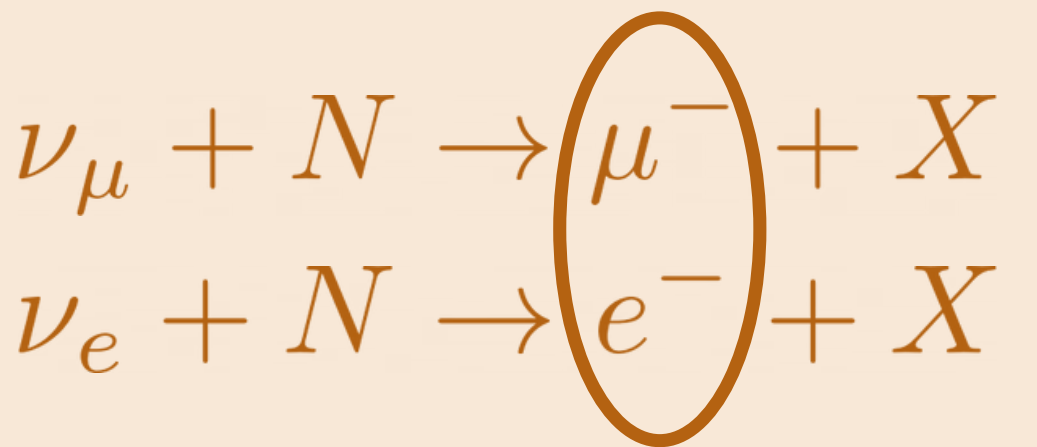
Based on the standard model of particle physics, we expect a 2:1 ratio of muon to electron neutrinos in the atmosphere.

$$\frac{\text{flux } \nu_\mu + \bar{\nu}_\mu}{\text{flux } \nu_e + \bar{\nu}_e} = 2 \text{ with 5% uncertainty across energy range (0.1 - 10)GeV}$$



Flux Ratio

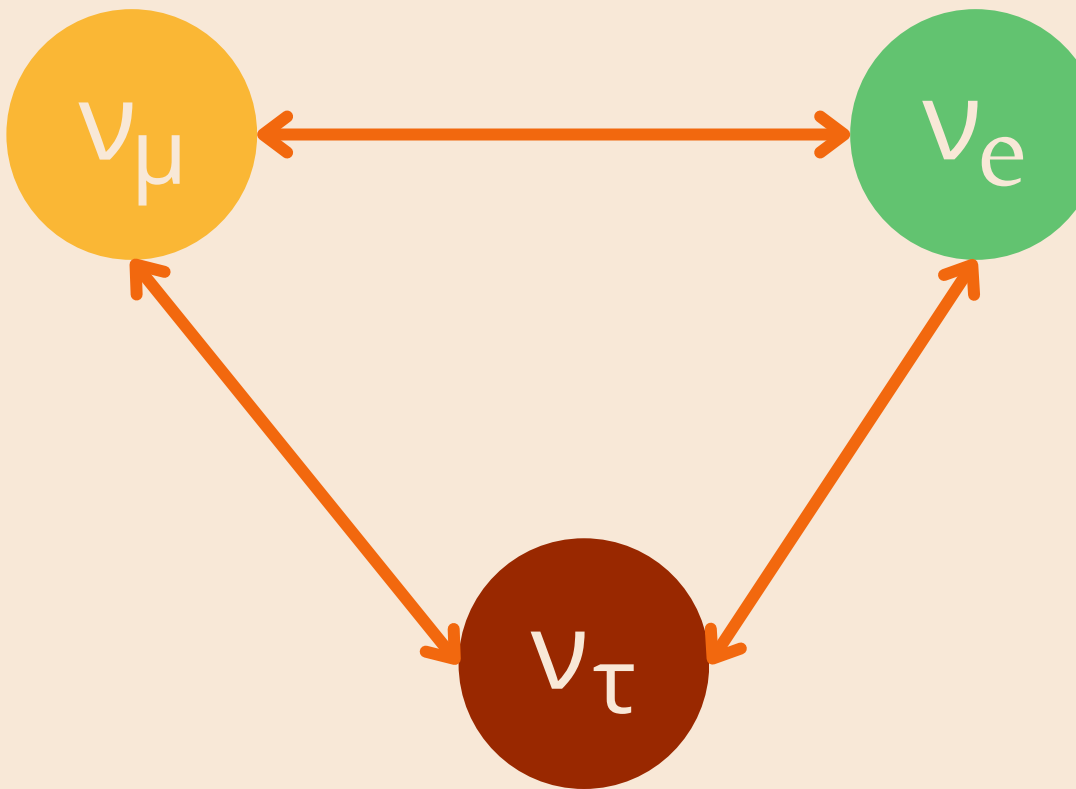
$\frac{\nu_\mu}{\nu_e}$ Calculated by observing leptons produced via charged-current interactions of neutrinos with nuclei.



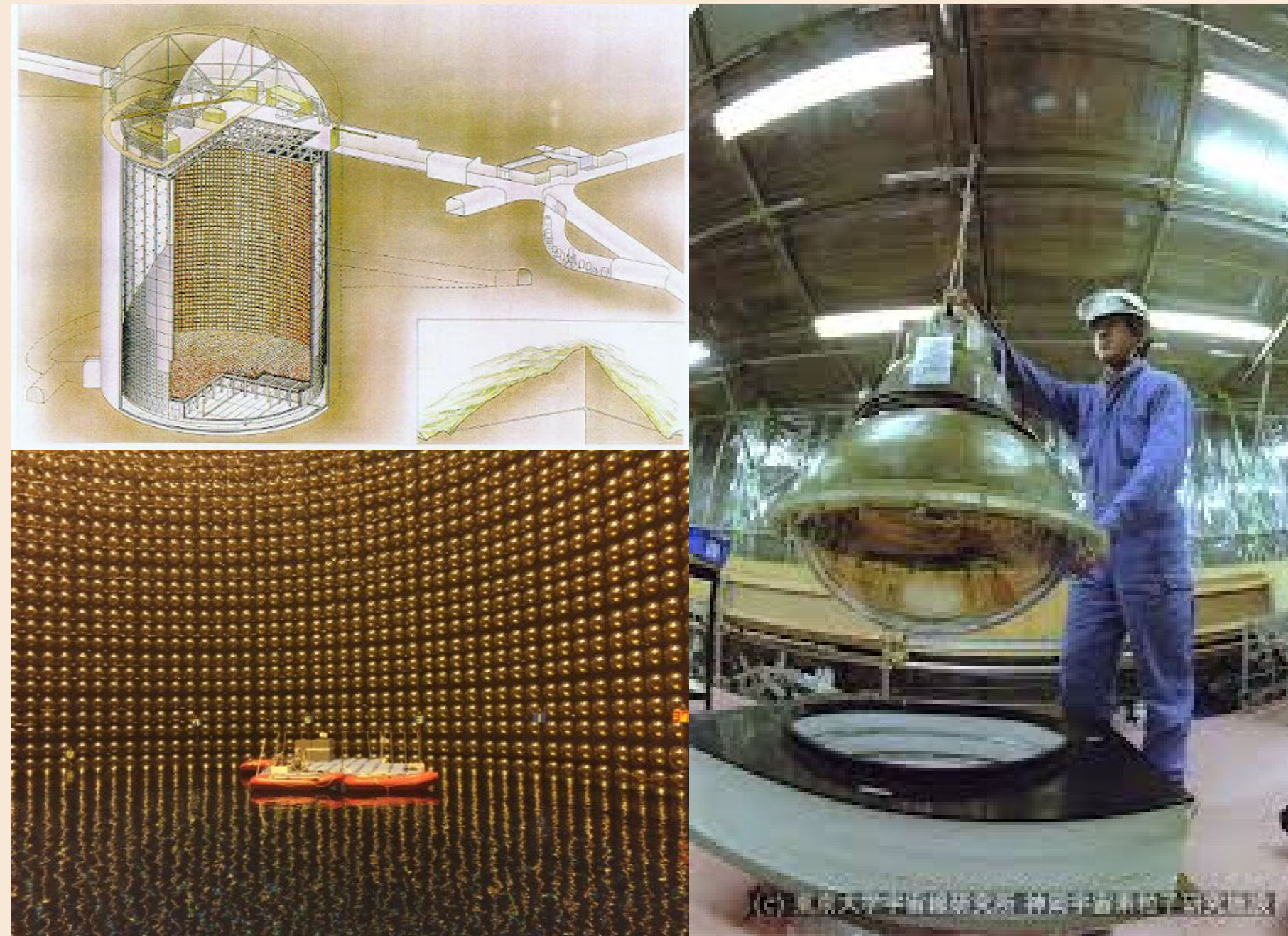
Neutrinos interact with the nuclei of atoms in matter, and the lepton that emerges from this interaction reveals the flavor of the neutrino.

Problem Statement

- Experiments detected fewer muon neutrinos than predicted.
- This discrepancy led to the hypothesis of neutrino oscillations.



Super-Kamiokande Detector



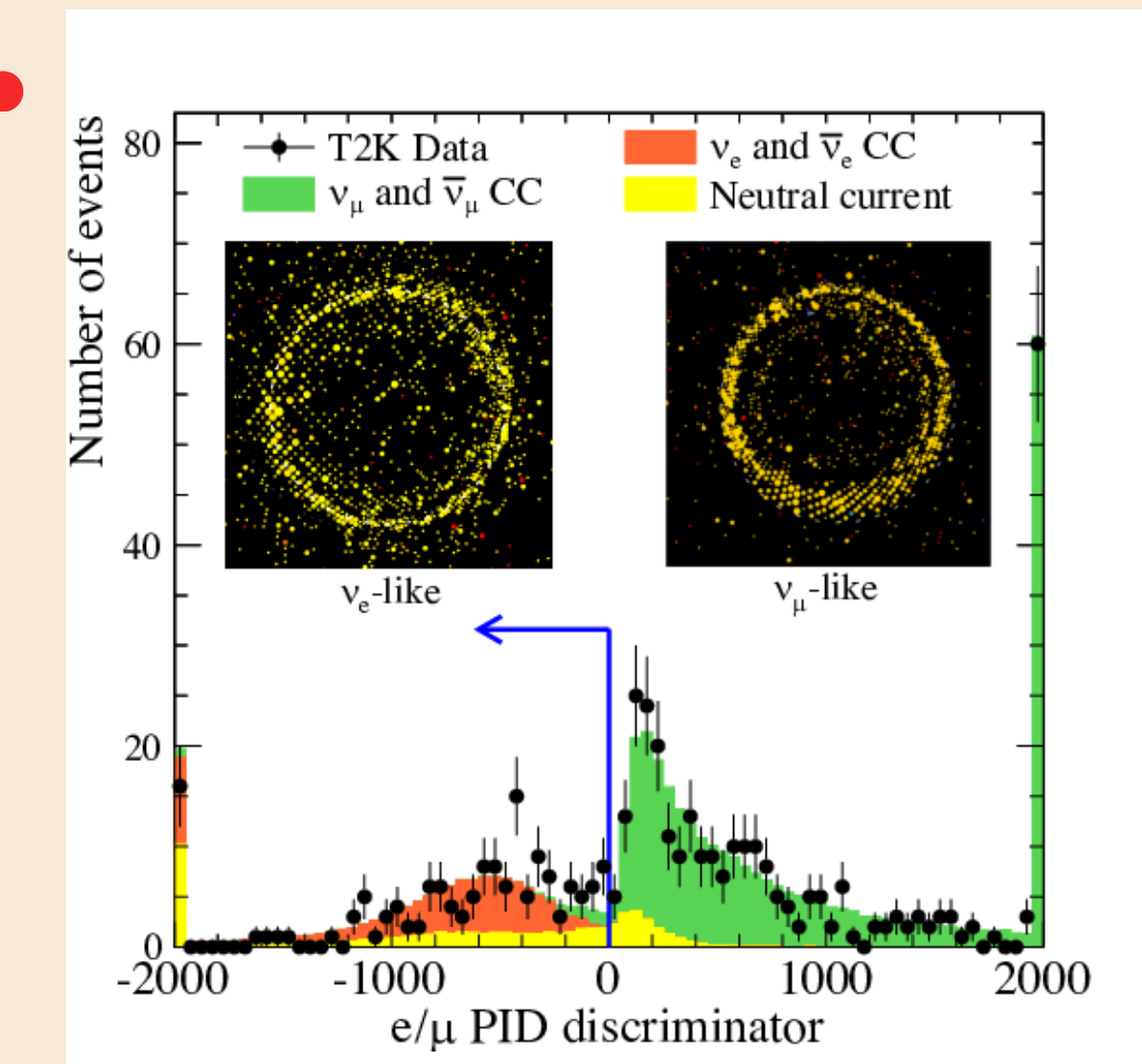
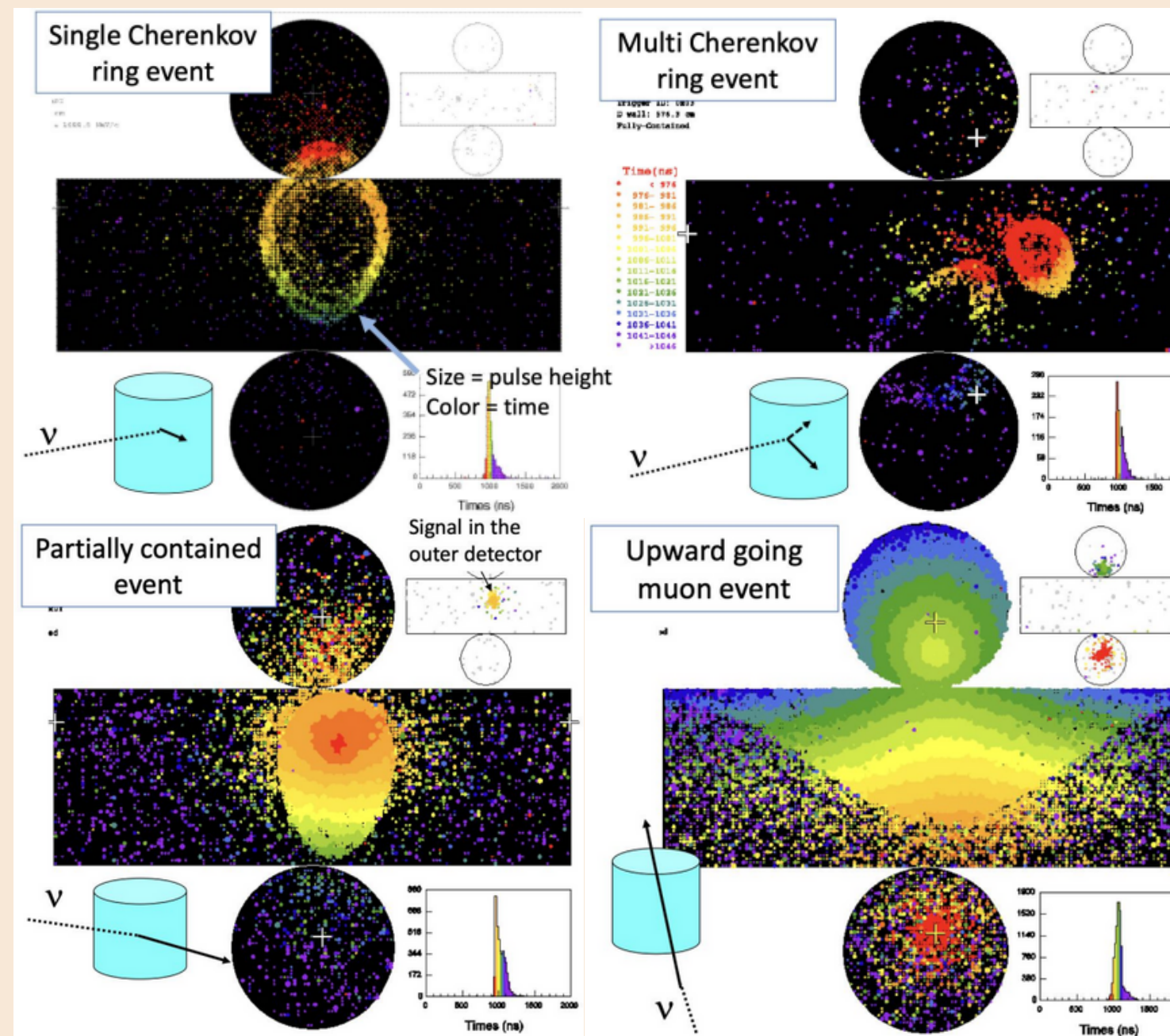
It is a 50 kton water Cherenkov detector

- 1000 m underground.
- 11146 photomultiplier tubes (PMTs).
- 22.5 kton fiducial volume of ultrapure water.
- Inner volume surrounded by a ~ 2 m thick outer detector with 1885 outward-facing PMTs.
- Outer detector used to veto entering particles and to tag exiting tracks.

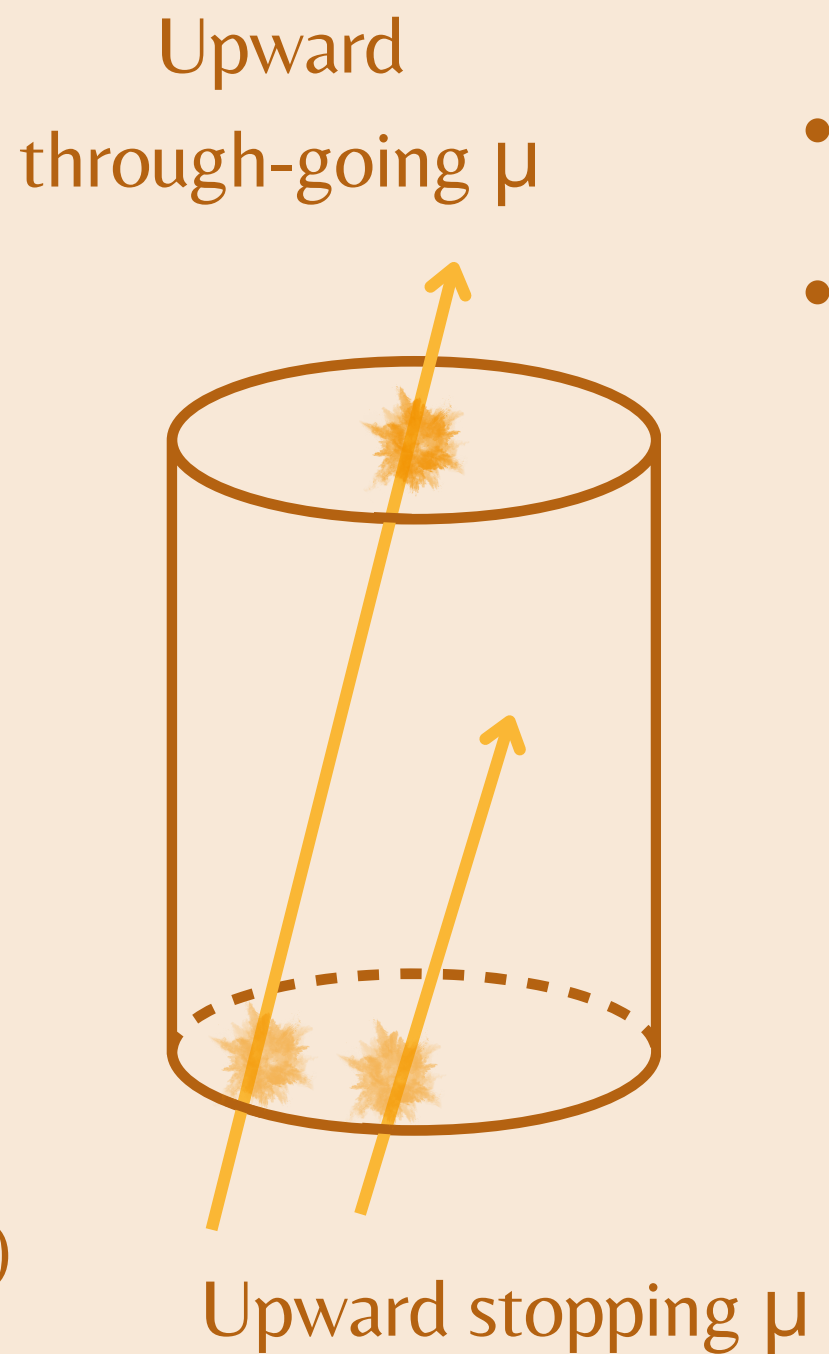
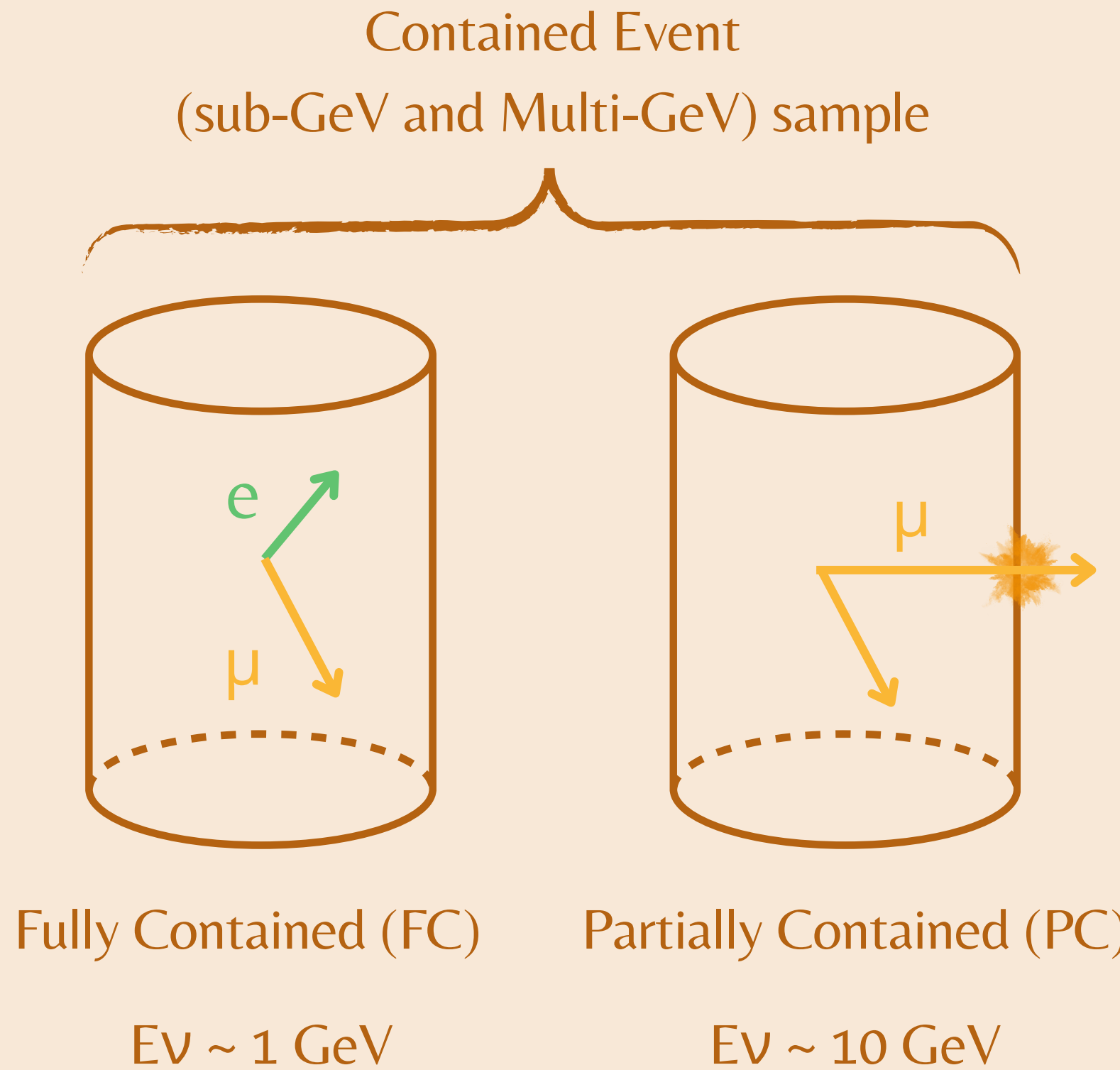
Cherenkov Light

When a neutrino interacts in the detector, it produces charged particles that move faster than the speed of light in water.

- This produce Cherenkov radiation, a cone of blue light, which is detected by the photomultipliers tubes inside the detector.

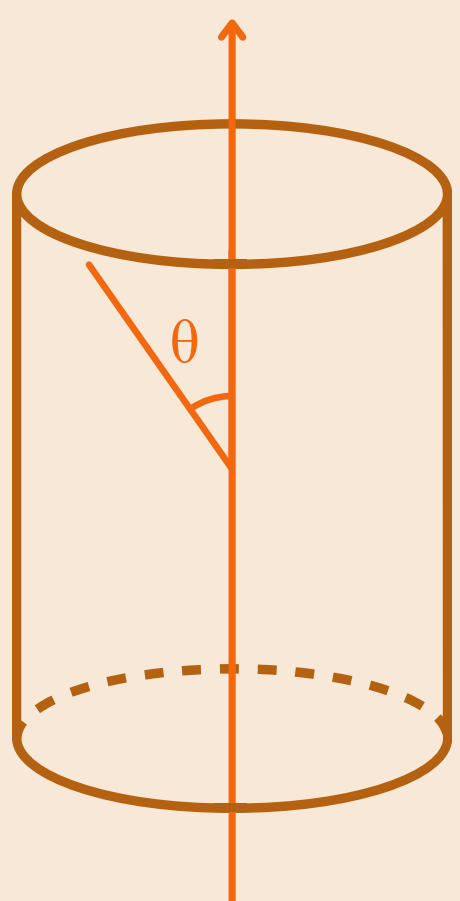
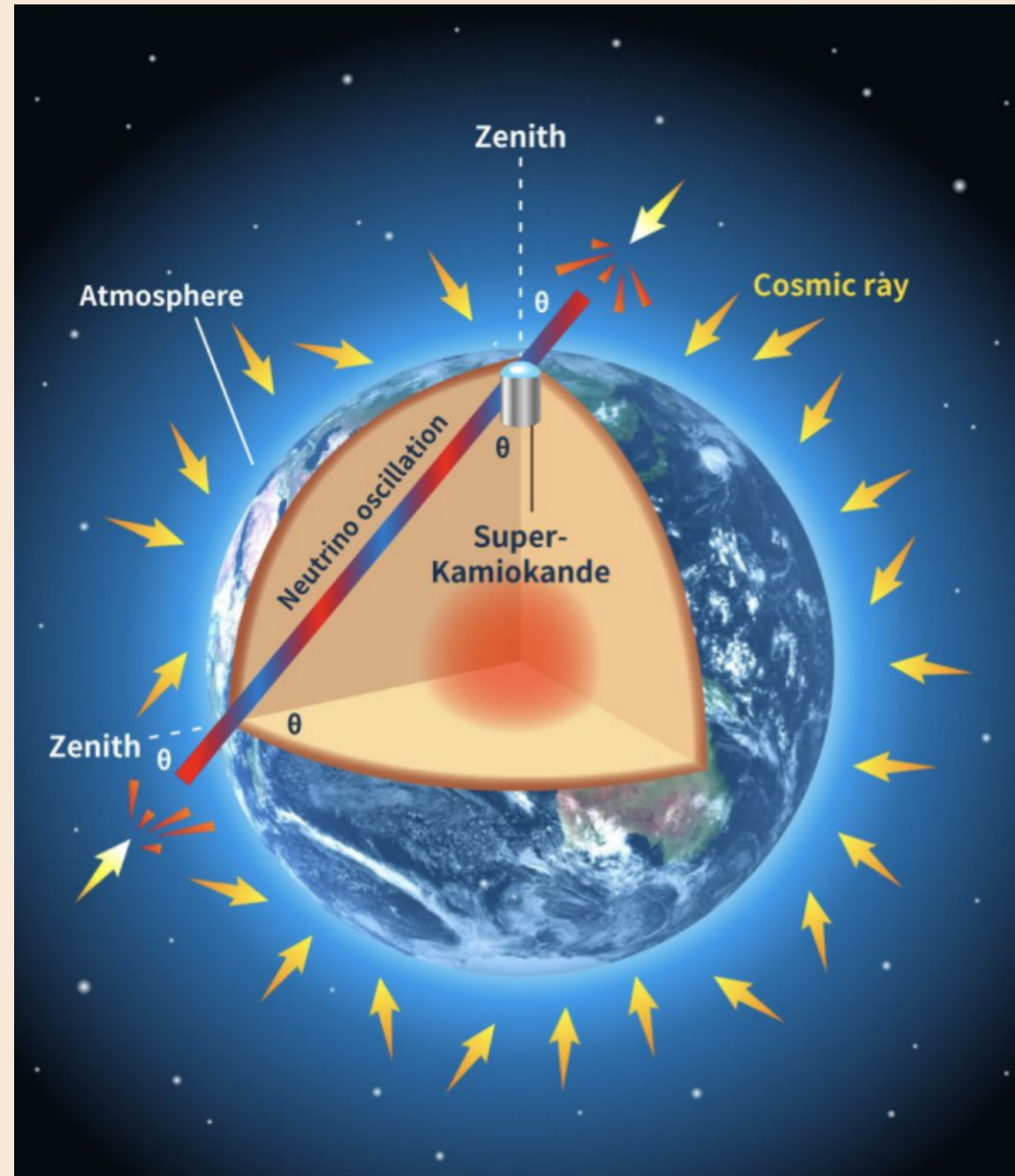


Data Adquisition



- 33.0 kton-year exposure.
- 535 days of data collection.
- Fully Contained (FC) and Partially Contained (PC) event types.

Zenith Angle Dependence



- Muon neutrino deficits are observed at large zenith angles (upward-going neutrinos).
- This deficit is a signature of neutrino oscillations.

Downward-going μ neutrinos
 $0^\circ < \theta < 78^\circ$

Upward-going μ neutrinos
 $101.5^\circ < \theta < 180^\circ$

R Measurement

$$R = \frac{(\mu/e)_{\text{DATA}}}{(\mu/e)_{\text{MC}}}$$

- R measures the ratio of muon to electron neutrinos compared to the predicted value.
- A smaller R indicates fewer muon neutrinos than expected.

TABLE I. Summary of the sub-GeV, multi-GeV, and PC event samples compared with the Monte Carlo prediction based on the neutrino flux calculation of Ref. [2].

	Data	Monte Carlo
Sub-GeV		
Single-ring	2389	2622.6
e -like	1231	1049.1
μ -like	1158	1573.6
Multi-ring	911	980.7
Total	3300	3603.3
$R = 0.63 \pm 0.03 \text{ (stat.)} \pm 0.05 \text{ (syst.)}$		
Multi-Gev		
Single-ring	520	531.7
e -like	290	236.0
μ -like	230	295.7
Multi-ring	533	560.1
Total	1053	1091.8
Partially contained	301	371.6
$R_{\text{FC+PC}} = 0.65 \pm 0.05 \text{ (stat.)} \pm 0.08 \text{ (syst.)}$		

Two-Flavor Neutrino Oscillation Model

For a two-neutrino oscillation hypothesis, the probability for a neutrino produced in flavor state a to be observed in flavor state b after traveling a distance L through a vacuum is:

$$P_{a \rightarrow b} = \sin^2 2\theta \sin^2 \left(\frac{1.27 \Delta m^2 (\text{eV}^2) L (\text{km})}{E_\nu (\text{GeV})} \right),$$

$E\nu$ = Neutrino energy.

θ = Mixing angle between the flavor eigenstates and the mass eigenstates.

Δm^2 = Mass squared difference between mass eigenstates.

Full flavor to neutrino mixing is described by PNSM matrix

$$\begin{pmatrix} \nu_e \\ \nu_\mu \\ \nu_\tau \end{pmatrix} = U_{\text{PMNS}} \begin{pmatrix} \nu_1 \\ \nu_2 \\ \nu_3 \end{pmatrix}$$

$$U_{\text{PMNS}} = \underbrace{\begin{pmatrix} 1 & 0 & 0 \\ 0 & \cos \theta_{23} & \sin \theta_{23} \\ 0 & -\sin \theta_{23} & \cos \theta_{23} \end{pmatrix}}_{\theta_{23}: \text{ Governs mixing between mass states } \nu_2 \text{ and } \nu_3 \text{ (atmospheric neutrinos)}} \underbrace{\begin{pmatrix} \cos \theta_{13} & 0 & e^{-i\delta} \sin \theta_{13} \\ 0 & 1 & 0 \\ -e^{i\delta} \sin \theta_{13} & 0 & \cos \theta_{13} \end{pmatrix}}_{\theta_{13}: \text{ Governs mixing between mass states } \nu_2 \text{ and } \nu_3 \text{ (allows three flavors mix)}} \underbrace{\begin{pmatrix} \cos \theta_{12} & \sin \theta_{12} & 0 \\ -\sin \theta_{12} & \cos \theta_{12} & 0 \\ 0 & 0 & 1 \end{pmatrix}}_{\theta_{12}: \text{ Governs mixing between mass states } \nu_1 \text{ and } \nu_2 \text{ (solar neutrinos)}}$$

θ_{23} : Governs mixing between mass states ν_2 and ν_3 (atmospheric neutrinos)

θ_{13} : Governs mixing between mass states ν_2 and ν_3 (allows three flavors mix)
CP violating phase

θ_{12} : Governs mixing between mass states ν_1 and ν_2 (solar neutrinos)

MC Simulations

$$N_{\text{MC}} = \frac{\mathcal{L}_{\text{DATA}}}{\mathcal{L}_{\text{MC}}} \sum_{\text{MC events}} w$$

$$w = (1 + \alpha) \left(\frac{E_\nu^i}{E_0} \right)^\delta (1 + \eta_{s,m} \cos \Theta) \\ \times f_{e,\mu} \left(\sin^2 2\theta, \Delta m^2, (1 + \lambda) \frac{L}{E_\nu} \right) \\ \times \begin{cases} (1 - \beta_s/2) & \text{sub-GeV } e\text{-like,} \\ (1 + \beta_s/2) & \text{sub-GeV } \mu\text{-like,} \\ (1 - \beta_m/2) & \text{multi-GeV } e\text{-like,} \\ (1 + \beta_m/2) \left(1 - \frac{\rho}{2} \frac{N_{PC}}{N_\mu}\right) & \text{multi-GeV } \mu\text{-like,} \\ (1 + \beta_m/2) \left(1 + \frac{\rho}{2}\right) & \text{PC.} \end{cases}$$

TABLE II. Summary of Monte Carlo fit parameters. Best-fit values for $\nu_\mu \leftrightarrow \nu_\tau$ ($\Delta m^2 = 2.2 \times 10^{-3} \text{ eV}^2$, $\sin^2 2\theta = 1.0$) and estimated uncertainties are given. (*) The overall normalization (α) was estimated to have a 25% uncertainty but was fitted as a free parameter.

	Monte Carlo fit parameters	Best fit	Uncertainty
α	Overall normalization	15.8%	(*)
δ	E_ν spectral index	0.006	$\sigma_\delta = 0.05$
β_s	Sub-GeV μ/e ratio	-6.3%	$\sigma_s = 8\%$
β_m	Multi-GeV μ/e ratio	-11.8%	$\sigma_m = 12\%$
ρ	Relative norm. of PC to FC	-1.8%	$\sigma_p = 8\%$
λ	L/E_ν	3.1%	$\sigma_\lambda = 15\%$
η_s	Sub-GeV up-down	2.4%	$\sigma_\eta^s = 2.4\%$
η_m	Multi-GeV up-down	-0.09%	$\sigma_\eta^m = 2.7\%$

μ -neutrino Deficit and Comparison to Models Without Oscillations

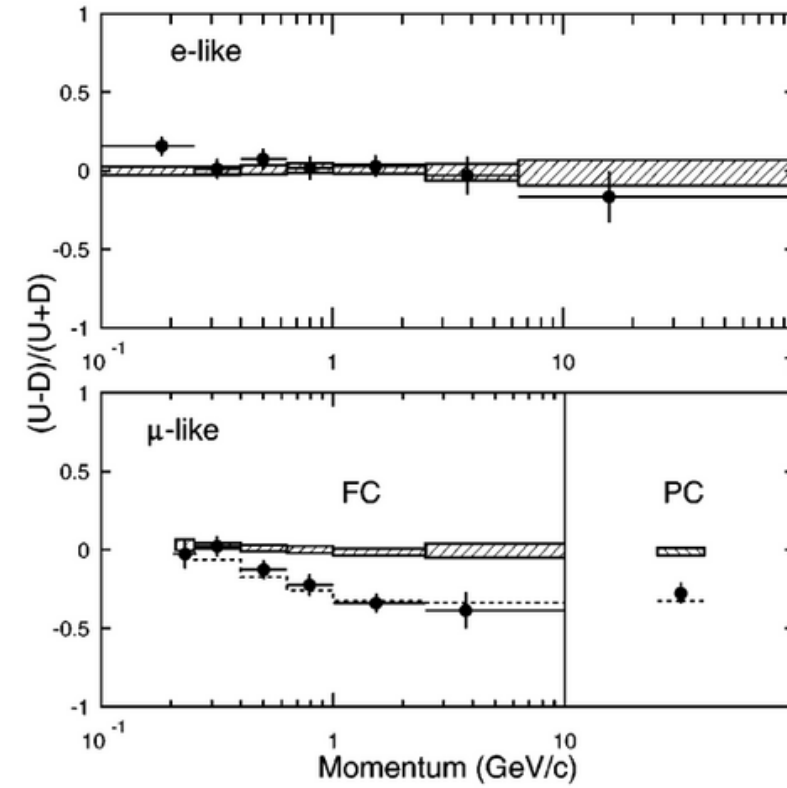


FIG. 1. The $(U - D)/(U + D)$ asymmetry as a function of momentum for FC e -like and μ -like events and PC events. While it is not possible to assign a momentum to a PC event, the PC sample is estimated to have a mean neutrino energy of 15 GeV. The Monte Carlo expectation without neutrino oscillations is shown in the hatched region with statistical and systematic errors added in quadrature. The dashed line for μ -like is the expectation for $\nu_\mu \leftrightarrow \nu_\tau$ oscillations with $(\sin^2 2\theta = 1.0, \Delta m^2 = 2.2 \times 10^{-3} \text{ eV}^2)$.

$\sin^2(2\theta)$ = Mixing angle, controls the amplitude of oscillation.

Δm^2 = Mass-squared difference, controls the oscillation frequency.

$$A = -0.296 \pm 0.048 \pm 0.01$$

$$\Delta A \sim 6\sigma!$$

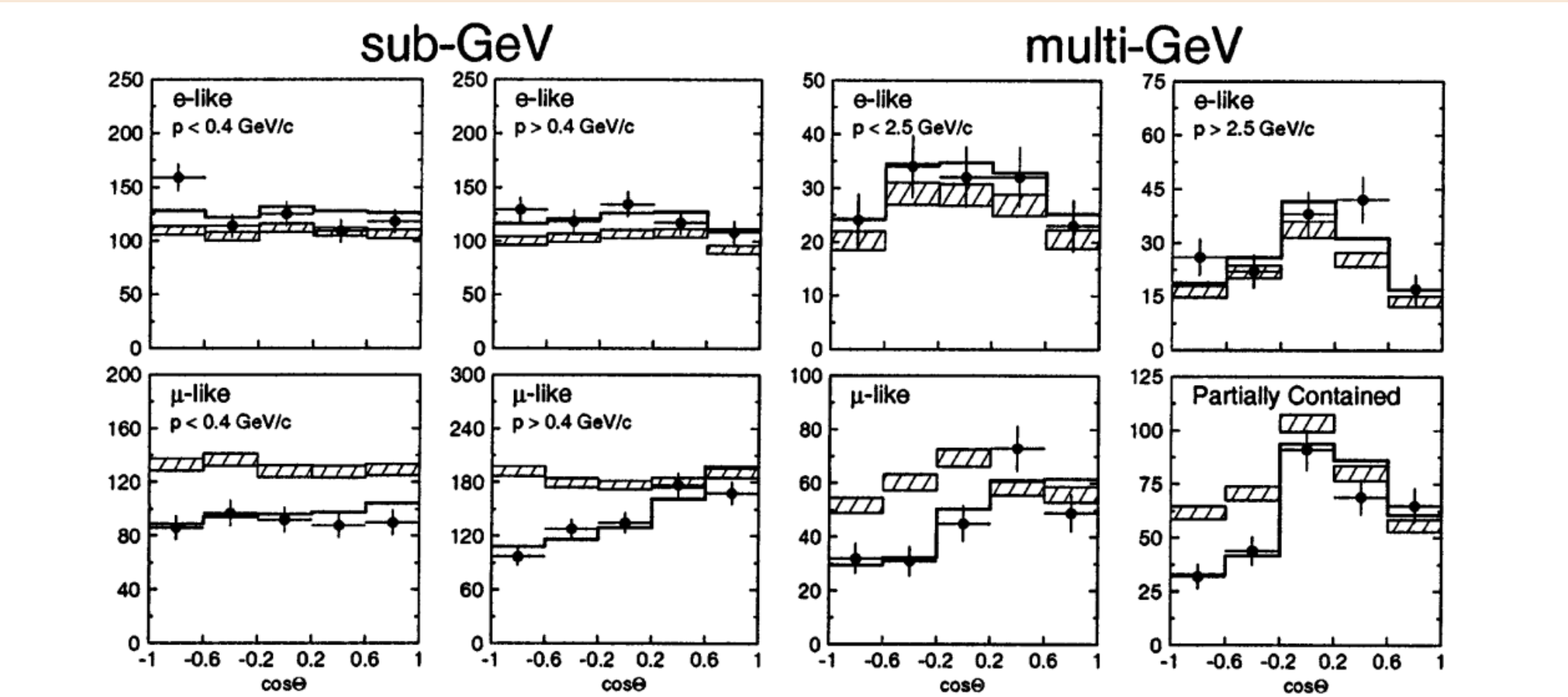


FIG. 3. Zenith angle distributions of μ -like and e -like events for sub-GeV and multi-GeV data sets. Upward-going particles have $\cos \Theta < 0$ and downward-going particles have $\cos \Theta > 0$. Sub-GeV data are shown separately for $p < 400 \text{ MeV}/c$ and $p > 400 \text{ MeV}/c$. Multi-GeV e -like distributions are shown for $p < 2.5$ and $p > 2.5 \text{ GeV}/c$ and the multi-GeV μ -like are shown separately for FC and PC events. The hatched region shows the Monte Carlo expectation for no oscillations normalized to the data live time with statistical errors. The bold line is the best-fit expectation for $\nu_\mu \leftrightarrow \nu_\tau$ oscillations with the overall flux normalization fitted as a free parameter.

χ^2 Comparison

A global scan was made on a $(\sin^2(2\theta), \log \Delta m^2)$ grid minimizing χ^2 .

$$\chi^2 = \sum_{\cos \Theta, p} \frac{(N_{\text{DATA}} - N_{\text{MC}})^2}{\sigma^2} + \sum_j \frac{\epsilon_j^2}{\sigma_j^2}$$

The number of observed events in the experimental data.

The number of predicted events from the MC simulation.

It is a statistical method used to compare the observed data to the expected results predicted by the neutrino oscillation model

Systematic errors (comes from uncertainties in neutrino flux, cross-section, and detector efficiency).

Uncertainties the systematic errors.

Statistical uncertainty, including data and MC uncertainties.

Confidence Intervals

$$\chi^2_{\min} = 65.2/67 \text{ DOF}$$

$$\sin^2(2\theta) = 1$$

$$\Delta m^2 = 2.2 \times 10^{-3} \text{ eV}^2$$

The best fits to μ -neutrino into τ -neutrino oscillations inside the physical region
 $0 < \sin^2(2\theta) < 1$

$$\chi^2_{\min} = 64.8/67 \text{ DOF}$$

$$\sin^2(2\theta) = 1.05$$

$$\Delta m^2 = 2.2 \times 10^{-3} \text{ eV}^2$$

Global minimum slightly outside of the physical region

$$\chi^2_{\min} = 135/69 \text{ DOF}$$

$$\sin^2(2\theta) = 0$$

$$\Delta m^2 = 0 \text{ eV}^2$$

Assuming no oscillations

$$\chi^2_{\min} = 87.8/67 \text{ DOF}$$

$$\sin^2(2\theta) = 0.93$$

$$\Delta m^2 = 3.2 \times 10^{-3} \text{ eV}^2$$

The best fits to μ -neutrino into e -neutrino oscillations

$$A_{\text{measured}} = -0.036 \pm 0.067 \pm 0.02$$

$$A = 0.205$$

$$\begin{aligned} 68\% &\rightarrow \chi^2_{\min} + 2.6 \\ 90\% &\rightarrow \chi^2_{\min} + 5.0 \\ 99\% &\rightarrow \chi^2_{\min} + 9.6 \end{aligned}$$

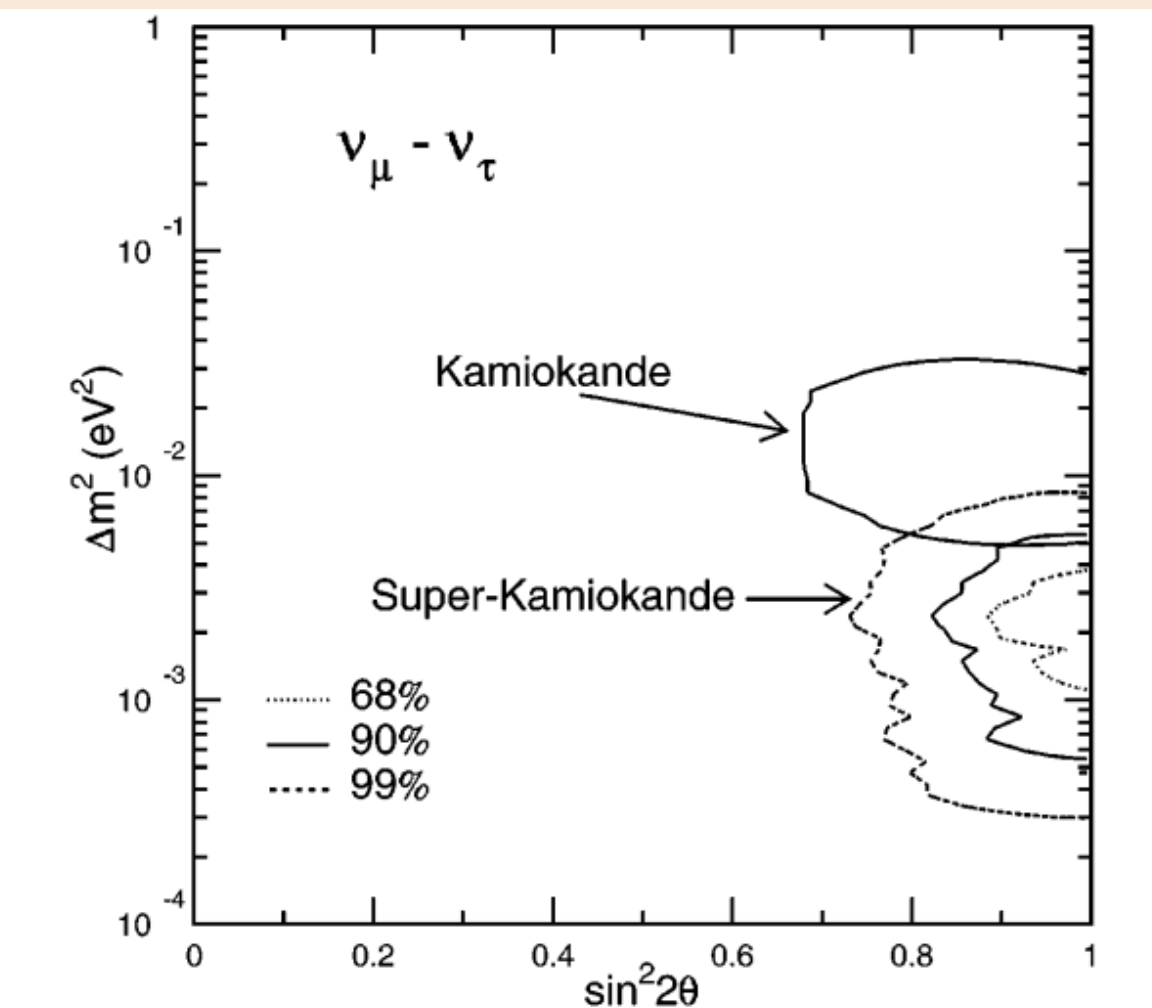


FIG. 2. The 68%, 90%, and 99% confidence intervals are shown for $\sin^2 2\theta$ and Δm^2 for $\nu_\mu \leftrightarrow \nu_\tau$ two-neutrino oscillations based on 33.0 kton yr of Super-Kamiokande data. The 90% confidence interval obtained by the Kamiokande experiment is also shown.

Final Evidence of Neutrino Oscillations

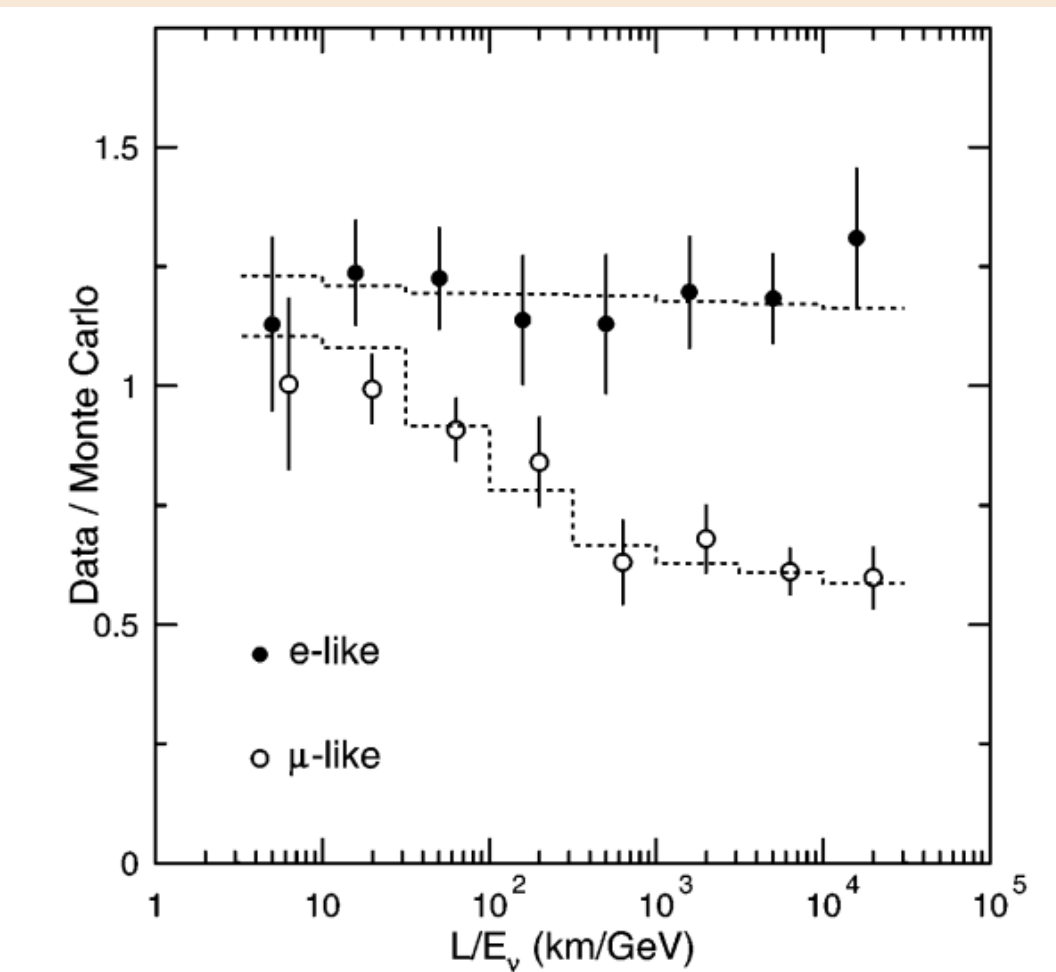


FIG. 4. The ratio of the number of FC data events to FC Monte Carlo events versus reconstructed L/E_ν . The points show the ratio of observed data to MC expectation in the absence of oscillations. The dashed lines show the expected shape for $\nu_\mu \leftrightarrow \nu_\tau$ at $\Delta m^2 = 2.2 \times 10^{-3} \text{ eV}^2$ and $\sin^2 2\theta = 1$. The slight L/E_ν dependence for e -like events is due to contamination (2–7%) of ν_μ CC interactions.

Conlcusions

- The evidence collected from Super-Kamiokande strongly supports muon neutrino oscillations into tau neutrinos.
- The evidence collected from Super-Kamiokande strongly supports muon neutrino oscillations into tau neutrinos.
- Sterile neutrinos may exist.



Thank you!

Bibliography

1. Kajita, T. (2017). Neutrino oscillations at the Super-Kamiokande detector [Video]. Emilio Segrè Lecture. Nobel Prize. Retrieved from https://www.youtube.com/watch?v=R3DPi9C_WSE and <https://www.nobelprize.org/uploads/2018/06/kajita-lecture-slides.pdf>
2. Hirata, K., Kajita, T., Koshiba, M., Nakahata, M., Oyama, Y., Sato, N., ... & Totsuka, Y. (1988). Experimental study of the atmospheric neutrino flux. Physics Letters B, 205(4), 416-420. [https://doi.org/10.1016/0370-2693\(88\)91690-5](https://doi.org/10.1016/0370-2693(88)91690-5)
3. Fukuda, Y., Hayakawa, T., Inoue, K., Ishihara, K., Ishino, H., Itow, Y., ... & Totsuka, Y. (1998). Evidence for oscillation of atmospheric neutrinos. Physical Review Letters, 81(8), 1562-1567. <https://doi.org/10.1103/PhysRevLett.81.1562>
4. Mueller, T. (2023, March 28). Super-Kamiokande: Oscillation analysis update [Conference presentation]. Thematic Workshop on Neutrinos, IN2P3. Retrieved from https://indico.in2p3.fr/event/28466/contributions/121380/attachments/76768/111414/SK_tmueller_kyoto_28March.pdf
5. Neutrino oscillations [Slide presentation]. (n.d.). SlidePlayer. Retrieved from <https://slideplayer.com/slide/10384372/>